MNRAS **000**, 1–4 (2019) Preprint 20 September 2019 Compiled using MNRAS LATEX style file v3.0

Lattice dynamics for a collisional dark matter fluid

Javier A. Acevedo-Barroso,[1]★ Jaime E. Forero-Romero,[1]†
[1]*Departamento de Física, Universidad de los Andes, Cra. 1 No. 18A-10 Edificio Ip, CP 111711, Bogotá, Colombia*

Accepted XXX. Received YYY; in original form ZZZ

ABSTRACT

TODO Usually, dark matter is simulated with N-body schemes that sample the phase space in order to solve the Poisson-Vlasov equation. This approach is heavily motivated by the ΛCMD cosmology, in which dark matter is a cold collisionless fluid. However, there is some evidence pointing towards self-interacting dark matter. Recent measurements on the aftermath of galaxy cluster collisions allow us to constrain the value of the thermally averaged cross section $\langle \sigma v \rangle$ of this self-interaction, thus motivating the development of dark matter *collisional* simulations.

On the other hand, Lattice Boltzmann simulations have been widely used to recreate increasingly complex fluids and boundary conditions, nonetheless, the usual Lattice-Boltzmann scheme does not simulate the entirety of the velocity space, but simply a small number of advective velocities.

In this work we implement a Lattice Boltzmann simulation of a collisional fluid. We implement a Lattice-Boltzmann simulations of the phase space of a *collisional* one dimensional dark matter fluid. For the collisional step, we use the BGK approximation modelled by a relaxation time τ chosen accordingly to recent estimates of the $\langle \sigma v \rangle$.

Key words: gravitation – methods: numerical – stars: kinematics and dynamics – galaxies: kinematics and dynamic – (cosmology:) dark matter

1 INTRODUCTION

In 2017 Mocz & Succi (2017) reintroduced a method originally proposed by Syer & Tremaine (1995) to simulate the evolution of the phase space of a collisionless stellar fluid. Their proposed method was symplectic, as defined in Earn & Tremaine (1992); Lagrangian; conservative; non-diffusive and time-reversible. The method consisted of solving the Poisson equation to calculate the gravitational potential at every time step, and then shifting density packets on the phase space lattice using a direct integration Euler scheme to calculate the new positions. The direct integration does not suffer from rounding error because of the use of integer arithmetic to update the positions on the phase space; however, the rounding of the acceleration does introduce an error, which is reduced as the resolution of the simulation increases. Overall, this method solves the discrete collisionless Boltzmann equation coupled with the discrete Poisson equation, but in the limit of high resolution, it converges to their continuous variants. Additionally, Mocz & Succi compared the method with traditional approaches such as N-body simulations using particle mesh, or finite volume schemes using a moving mesh; and found that their method is a very computationally cheap alternative, and considerably better at resolving fine structure in the phase space. The main drawback of the method comes from the memory requirements of the direct integration, as it scales as $N_x^D N_v^D$, where D is the number of spatial dimensions. In this work we used $D = 1$. Thus allowing for a very high resolution.

On the other hand, Lattice Boltzmann methods (LBM) solve the discrete Boltzmann equation by dividing it in two different steps: the streaming step, where the phase space lattice is updated according to the collisionless Boltzmann equation; and the collisional step, where the phase space is updated according to a particular collisional operator, usually the Bhatnagar-Gross-Krook (BGK) operator (Bhatnagar et al. 1954). However, the most common approach uses only a small number of advective velocities instead of the whole velocity space. The method reintroduced in Mocz & Succi (2017) can be interpreted as the streaming step of a LBM –renamed as kick– with the addition of a 'drift' step to account for the changes in the velocity space.

Here, we reproduce Mocz & Succi method and extend it by adding a collisional relaxation during the kick step modelled by the BGK operator. The result is a LBM that is capable of simulating stellar fluids regardless of their collisional nature.

★ E-mail: ja.acevedo12@uniandes.edu.co
† E-mail: je.forero@uniandes.edu.co

2 THE BOLTZMANN EQUATION

The state of a fluid can be described by the phase space density $f(\boldsymbol{r}, \boldsymbol{v}; t)$, which gives the density of stellar fluid in the position $\boldsymbol{r}$ with velocity $\boldsymbol{v}$. The mass density is calculated by integration of the phase space density over the entire velocity space:

$$\rho(\boldsymbol{r}; t) = \int f(\boldsymbol{r}, \boldsymbol{v}; t)\, \mathrm{d}^3\mathbf{v}\,. \tag{1}$$

The evolution of the phase space density is modeled by the Boltzmann equation:

$$\frac{\partial f}{\partial t} + \boldsymbol{v} \cdot \frac{\partial f}{\partial \boldsymbol{r}} - \frac{\partial \Phi}{\partial \boldsymbol{r}} \cdot \frac{\partial f}{\partial \boldsymbol{v}} = C[f]. \tag{2}$$

Where Φ denotes the gravitational potential. The homogeneous solution to the left hand side corresponds to the collisionless Boltzmann equation – also known as the Vlasov equation –, which is often used to simulate self-gravitating collisionless stellar systems (Springel, Yoshida & White 2001; Yoshikawa, Yoshida & Umemura 2013; Hahn & Angulo 2016; Mocz & Succi 2017). The right hand side corresponds to the collisional operator, and quantifies the effect of collisions during the evolution of the phase space. Under the assumption of molecular equilibrium, C is formally given by (Succi 2001):

$$C[f] = \int g I(g, \Omega)[f'_{\mathrm{a}} f'_{\mathrm{b}} - f_{\mathrm{a}} f_{\mathrm{b}}]\mathrm{d}\Omega \mathrm{d}^3\boldsymbol{v}_{\mathrm{a}} \tag{3}$$

where Ω denotes the solid angle, $I(g, \Omega)$ the differential cross section for a pair of particles with relative velocity $\boldsymbol{g} = g\boldsymbol{\Omega}$, $f_{\mathrm{i}} = f(\boldsymbol{r}, \boldsymbol{v}_{\mathrm{i}}; t)$ represents the mass densities before the collisions, and $f'_{\mathrm{i}} = f(\boldsymbol{r}, \boldsymbol{v}'_{\mathrm{i}}; t)$ represents the densities after the collisions. The formal modelling of the collisional operator links the macroscopic effects with the microscopic world using the differential cross section I, which requires knowledge of the short range interactions between particles. In order to keep the simulation general enough, we work with the BGK approximation. The BGK operator quantifies collisions as a relaxation process towards *local equilibrium* modelled by a relaxation time τ:

$$C[f] = -\frac{(f - f^{\mathrm{e}})}{\tau}, \tag{4}$$

where f^{e} represents the local equilibrium distribution. In this work we use a Maxwell-Boltzmann equilibrium. The details of the implementation are expanded in 3.2.

Lastly, in order to account for the gravitational interaction, the Boltzmann equation is coupled with the Poisson equation:

$$\nabla^2\Phi(\boldsymbol{r}; t) = 4\pi G\rho(\boldsymbol{r}; t). \tag{5}$$

3 LATTICE BOLTZMANN METHOD (LBM)

The usual Lattice-Boltzmann method divides the phase space density into a lattice, and solves the discrete Boltzmann equation in two steps: the free streaming step and the collisional step. However, those steps do not account for the evolution of the velocity space, and thus we choose to divide our implementation of LBM in a 'kick' step, and a 'drift' step as proposed by Mocz & Succi (2017). Finally, to account for the collisions, we do not implement a complete collisional step, but add a collisional relaxation to the 'kick' step. We worked with simulations of dimensionality 1+1, and so, our description of the algorithm is done for a one dimensional fluid. None the less, is readily extendable to two and three spatial dimensions. We explain the collisionless version of the LBM in section 3.1, and the collisional modifications in section 3.2.

3.1 Collisionless method

In the lattice, $f(x, v; t)\Delta x\Delta v$ corresponds to the mass of fluid with positions in the range $[x, x+\Delta x]$ and velocities in the range $[v, v+\Delta v]$ during the instant t, where Δx and Δv is the separation between lattice nodes for the position and velocity dimensions respectively. The boundary values of the phase space and set of physical units are chosen particularly for each system to simulate.

The first step is to initialize the phase space according to the system of interest. Then, integrate the velocity space to obtain the density profile. Due the lattice, integration become a sum over the entire velocity grid:

$$\rho(x; t) = \sum_{v=v_{\mathrm{min}}}^{v_{\mathrm{max}}} f(x, v; t)\Delta v. \tag{6}$$

With the physical density profile, we solve the Poisson equation applying the pseudo-spectral method, as proposed by Fuka (2014), and use the Fastest Fourier Transform of the West implementation of the Fast Fourier Transform (Frigo & Johnson 2005). We perform a central difference numerical derivative on the gravitational potential to obtain the acceleration profile and from then, we proceed to update the phase space lattice. In the collisionless case, the update is done in two steps: the 'kick' step, and the 'drift' step. The kick step is the update of the spatial position of the fluid. Let (nx_i, nv_i) be the *integer* positions in the lattice corresponding to (x_i, v_i) in $f(x, v; t)$, then the new spatial integer position nx_f of x_f is given by:

$$nx_f = nx_i + \lfloor v\Delta t/\Delta x \rceil, \tag{7}$$

where $\lfloor . \rceil$ represents the round-to-nearest integer operator. Likewise, the drift step is the update of the velocity space. The new velocity integer position nv_f of v_f is given by:

$$nv_f = nv_i + \lfloor a\Delta t/\Delta v \rceil. \tag{8}$$

The updated lattice after both steps is given by:

$$f(x_f, v_f; t + \Delta t) = f(x_i, v_i; t) \tag{9}$$

Once updated the phase space, we recalculate density, and the loop continues from there.

3.2 Collisional modifications

3.2.1 *The local equilibrium function*

To define the collisional modifications, first we must define an equilibrium function f^{e}. Such function must ensure mass, moment and energy conservation, and comply to $C[f^{\mathrm{e}}] = 0$ (Succi 2001). Therefore, due equation 2:

$$f^{\mathrm{e}\prime}_{\mathrm{a}} f^{\mathrm{e}\prime}_{\mathrm{b}} = f^{\mathrm{e}}_{\mathrm{a}} f^{\mathrm{e}}_{\mathrm{b}}, \tag{10}$$

and,

$$\ln f^{\mathrm{e}\prime}_{\mathrm{a}} + \ln f^{\mathrm{e}\prime}_{\mathrm{b}} = \ln f^{\mathrm{e}}_{\mathrm{a}} + \ln f^{\mathrm{e}}_{\mathrm{b}}. \tag{11}$$

Which can be interpreted as $\ln(f^{\mathrm{e}})$ being a quantity conserved during collisions. The most important consequence is that f^{e} must be a linear combination of dynamically conserved functions, such as the linearly independent set: $\{1, v, v^2/2\}$, mass conservation, momentum conservation and energy conservation. As a result, f^{e} obeys:

$$\ln f^{\mathrm{e}} = A + Bv + \frac{1}{2}Cv^2, \tag{12}$$

and the parameters A, B, C are Lagrangian multipliers obtained by imposing the conservation of mass $\rho(x)$, momentum $u(x)$ and energy $\varepsilon(x)$. The quantity $\rho(x)$ is given by equation 6, $u(x)$ and ε are given by:

$$\rho(x;t)u(x;t) = \sum_{v=v_{\min}}^{v_{\max}} v f(x,v;t)\Delta v, \tag{13}$$

$$\rho(x;t)\varepsilon(x;t) = \sum_{v=v_{\min}}^{v_{\max}} \frac{v^2}{2} f(x,v;t)\Delta v. \tag{14}$$

In the end, we express f^{e} as (Asinari 2005):

$$f^{e}(x,v) = \frac{\rho(x;t)}{\sqrt{2\pi\varepsilon(x;t)}} \exp\left[-\frac{(u(x;t)-v)^2}{2\varepsilon(x;t)}\right], \tag{15}$$

which is simply the Maxwellian distribution.

3.2.2 *Modified kick step*

Once defined the equilibrium function f^{e}, we can use equation 4 and the language from the last subsection to define a modified kick step:

$$f(x_f, v_f; t+\Delta t) = f(x_i, v_f; t) - \frac{1}{\tau}\left[f(x_i, v_f; t) - f^{\mathrm{e}}(x_i, v_f)\right]. \tag{16}$$

Note that we perform the drift step before the kick step.

4 RESULTS

The main effect of the discretization of the phase space is that we no longer use the entire phase space, but a discrete number of velocities and positions, which allows for the use of integer arithmetic when updating the lattice. This eliminates the floating point error but introduces lattice noise during the discretization of the acceleration. In the limit of high resolution, the absence of floating point error and the tendency of the lattice noise towards zero guarantees that the method converges to the continuum solution of the Boltzmann equation. Overall, the algorithm recovers the Euler-Lagrange equations and conserves mass, momentum and energy

TODO.

5 NUMERICAL TESTS

In this section we present a series of numerical tests using our implementation of the method in order to demonstrate its capacity to simulate both collisionless and collisional stellar fluids.

5.1 Test I: Gaussian Landau dampening

We initialize the phase space grid with a Gaussian distribution given by:

$$f(x,v,t=0) = 4exp(-\frac{-x^2-v^2}{0.08}), \tag{17}$$

in a two dimensional phase space defined by $x \in [-1,1]$ and $v \in [-1,1]$. The biggest concentration of mass is on the spatial origin, therefore the potential minima is also on the origin. A matter package initially in a lattice cell representing a positive velocity will move in the positive direction of the spatial axis, negative velocities will move in the negative direction. At the same time, moving towards the potential minima increases rapidity, doing the opposite decreases rapidity. The overall effect is the development of thin arms that turn into a spiral. Eventually, the spiral converges to a semi-stable distribution. Depending on the resolution of the simulation, the final state of the phase space looks like a very dense spiral, or a cloudy distribution. Since we are working in a two dimensional phase space, we are not limited by memory constrains. We use a lattice of size 2048^2, thus being able to resolve the fine arm structure even at very later times. This test originated from Alard & Colombi (2005), who used it to test a cloudy Vlasov-Poisson solver, and has also being used by Colombi & Touma (2014) and Mocz & Succi (2017) to test a waterbag solver and the collissionless version of this method respectively.

We ran simulations with $\tau = \{500, 8727, \infty\}$, $\tau \to \infty$ corresponds to a collisionless run. The results for a couple selected times can be observed in figure 1. The thin arm structure is effectively resolved at time $t = 5$ and the semi-stable spiral at time $t = 20$. Both structures are present regardless of the relaxation time τ; however, the extend of the spiral is reduced as τ decreases.

5.2 Test II: Jeans Instability

We initialize the phase space grid with a uniform density ($\bar{\rho}$) along with a small periodic spatial perturbation and a Gaussian velocity profile:

$$f(x,v,t=0) = \frac{\bar{\rho}}{(2\pi\sigma^2)^{1/2}} \exp\left(-\frac{(v-u)^2}{2\sigma^2}\right)(1 + A\cos(kx)). \tag{18}$$

Where A and k are respectively the amplitude and frequency of the perturbation, u is the mean velocity, and σ is the velocity dispersion. The phase space is defined by $x \in [-L/2, L/2]$ and $v \in [-V, V]$. The idea behind this initialization is to trigger either the Jeans instability or Landau Dampening. The dynamics of the system is determined by the ratio k/k_j with k_j given by:

$$k_j^2 = \frac{4\pi G\bar{\rho}}{\sigma^2}. \tag{19}$$

If $k/k_j < 1$, the perturbations will trigger the Jeans instability and grow. If $k/k_j > 1$, the perturbations will be erased by Landau dampening. We present results for $k/k_j = 0.5, 1.5$ and study the time evolution of the system. The dynamical time of the system is defined by:

$$T = (G\bar{\rho})^{-1/2}, \tag{20}$$

and it relates to the phase space domain by $V = L/T$. Without loss of generality, we fix $L = T = 1$, thus $V = 1$. Additionally, we fix the mean velocity $u = 0$. Due the periodic boundary conditions on the spatial axis, we must ensure continuity on the boundaries, and thus:

$$k = \frac{2\pi n}{L}. \tag{21}$$

We chose $n = 2$, fix the amplitude of the perturbation $A = 0.03$, and calculate the velocity dispersion σ accordingly.

5.3 Test III: Galilean invariance

Given the symplectic and Lagragian nature of the method, we expect it to assure Galilean invariance. To test it, we initialize the system in a Jeans instability with the same parameters as in section 5.2 but using different mean velocity u. We ran simulations with $u = \{0, \sigma, 2\sigma\}$, for $k/k_j = 0.5$ and $k/k_j = 1.1$. However, due the

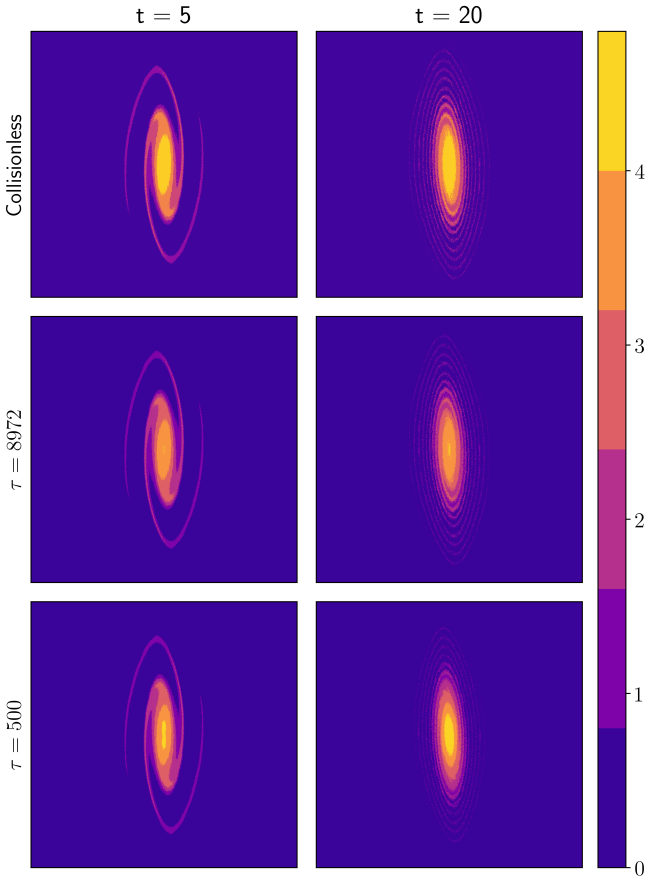

Figure 1. Numerical test of Landau dampening for Gaussian initial conditions. We ran simulations with different values of τ. All units are simulation units and have not being scaled for any astrophysical system in particular. It is easy to observe the thin arm structure mentioned in section 5.1

.

boundary conditions on the velocity space we must reduce σ in order to keep the Due the periodicity of the perturbation, its size $\delta(x)$ is quantified by:

$$\delta(x) = \frac{\rho(x) - \bar{\rho}}{\bar{\rho}}, \tag{22}$$

and in terms of its Fourier power series:

$$\delta(x) = \sum_{m \geq 0} A_m \exp(2i\pi m x / L). \tag{23}$$

Since we chose $n = 2$ in k, the evolution of the second Fourier coefficient (A_2) will quantify the evolution of the initial perturbation, regardless of the phase of the wave. We observe for both $k/k_j = 0.5$ (figure 5.3) and $k/k_j = 1.1$ (figure **??**) that regardless of the value of u the evolution of the Fourier coefficient is the same, therefore the behavior of the perturbation is independent of the mean velocity of the system. Thus, successfully testing Galilean invariance.

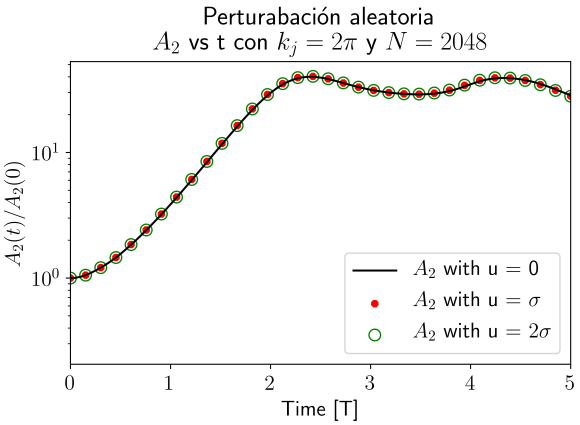

6 CONCLUSIONS

TODO

ACKNOWLEDGEMENTS

TODO

REFERENCES

Alard C., Colombi S., 2005, MNRAS, 359, 123
Asinari P., 2005, PhD thesis, Politecnico di Torino
Bhatnagar P. L., Gross E. P., Krook M., 1954, Physical Review, 94, 511
Colombi S., Touma J., 2014, MNRAS, 441, 2414
Earn D. J. D., Tremaine S., 1992, Physica D Nonlinear Phenomena, 56, 1
Frigo M., Johnson S. G., 2005, Proceedings of the IEEE, 93, 216
Fuka V., 2014, arXiv e-prints, p. arXiv:1409.8116
Hahn O., Angulo R. E., 2016, MNRAS, 455, 1115
Mocz P., Succi S., 2017, MNRAS, 465, 3154
Springel V., Yoshida N., White S. D. M., 2001, New Astron., 6, 79
Succi S., 2001, The Lattice Boltzmann Equation for Fluid Dynamics and Beyond (Numerical Mathematics and Scientific Computation). Oxford University Press, USA
Syer D., Tremaine S., 1995, MNRAS, 276, 467
Yoshikawa K., Yoshida N., Umemura M., 2013, ApJ, 762, 116

This paper has been typeset from a TEX/LATEX file prepared by the author.